HAL
open science

Line of Sight controller tuning using Bayesian optimization of a high-level optronic criterion

Sophie Frasnedo, Julien Bect, Cédric Chapuis, Gilles Duc, Philippe Feyel, Guillaume Sandou

To cite this version:

Sophie Frasnedo, Julien Bect, Cédric Chapuis, Gilles Duc, Philippe Feyel, et al.. Line of Sight controller tuning using Bayesian optimization of a high-level optronic criterion. 16th IFAC Workshop on Control Applications of Optimization, Oct 2015, Garmisch-Partenkirchen, Andorra. pp.56-61, 10.1016/j.ifacol.2015.11.059 . hal-01259423

HAL Id: hal-01259423

https://centralesupelec.hal.science/hal-01259423v1

Submitted on 1 Aug 2017

HAL is a multi-disciplinary open access archive for the deposit and dissemination of scientific research documents, whether they are published or not. The documents may come from teaching and research institutions in France or abroad, or from public or private research centers.

L'archive ouverte pluridisciplinaire **HAL**, est destinée au dépôt et à la diffusion de documents scientifiques de niveau recherche, publiés ou non, émanant des établissements d'enseignement et de recherche français ou étrangers, des laboratoires publics ou privés.

Line of Sight controller tuning using Bayesian optimization of a high-level optronic criterion

S. Frasnedo [*,**] **J. Bect** [*] **C. Chapuis** [**] **G. Duc** [*] **Ph. Feyel** [**] **G. Sandou** [*]

[*] *Laboratoire des Signaux et Systèmes (L2S, UMR CNRS 8506), CentraleSupélec - CNRS -Université Paris-Sud, 3 rue Joliot-Curie, 91192 Gif-sur-Yvette, France (e-mail: {sophie.frasnedo, julien.bect, gilles.duc, guillaume.sandou}@centralesupelec.fr*
[**] *Sagem Defence and Security (Safran), France (e-mail: {sophie.frasnedo, cedric.chapuis, philippe.feyel}@sagem.com)*

Abstract: A method to globally optimize the parameters of the controller of an inertially stabilized platform is presented. This platform carries an electro-optical system. The quality of the produced image is obviously influenced by the capacity of the controller to compensate for the unwanted motion of the platform. The motion Modulation Transfer Function (motion MTF) measures the amount of blur brought into the image by those parasite movements. The controller is tuned by minimizing a criterion which includes the motion MTF. However, evaluating this criterion is time-consuming. Using an optimization method that needs numerous evaluations of the criterion is not compatible with industrial constraints. Bayesian optimization methods consist in combining prior information about the criterion and previous evaluation results in order to choose efficiently new evaluation points and reach the global minimizer within a reasonable time. In this paper, a Bayesian approach is used to optimize the motion MTF-based criterion. The results are compared with a local optimization of the same MTF-based criterion, initialized with an acceptable initial point. Similar performances are achieved by the proposed methodology, without requiring an initialization point.

Keywords: Expensive to evaluate functions, Global optimization, Image motion compensation, Inertial Platform, Modulation Transfer Function, Parameter optimization

1. INTRODUCTION

The image quality of an electro-optical system such as an Inertially Stabilized Platform (ISP) can be measured using the Modulation Transfer Function (MTF). The MTF represents the degradation of the contrast over spatial frequencies (see Holst (2008)). Several phenomena contribute to the image degradation and each of them is associated with an MTF. The system MTF is the product of these elementary incoherent MTFs. In the Line of Sight (LoS) stabilization field, the quantity of interest is the motion MTF.

1.1 The considered plant

The LoS is the direction an optical sensor is aiming at. The role of the ISP is to hold the LoS of the optical sensor relative to inertial space. Missile guidance and astronomical telescopes are examples of ISP applications (Hilkert (2008)). The system considered here consists of two orthogonal gimbals allowing two rotations in pitch and yaw, see Fig. 1. These two rotations are supposed to isolate the imager from the external movements of the platform. Nevertheless, in spite of a careful mechanical design, disturbances appear. A feedback loop including a gyrometer is thus added to each rotational axis to counter

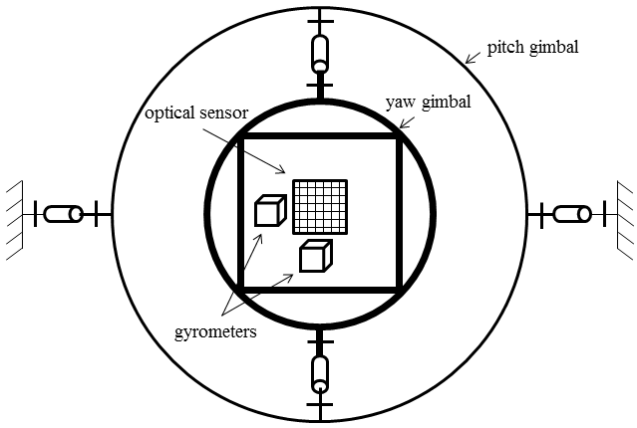

Fig. 1. Drawing of the studied ISP (two rotational axes)

these disturbances. Both the imager and the gyrometer are mounted directly on the inner gimbal. For sake of simplicity, the two rotational movements are considered to be decoupled. Thus, only the rotation in pitch is studied in the sequel.

The block diagram in Fig. 2 shows the model of the system used for the study: ω_{ref} is the absolute rate reference input. For our stabilization application, it is

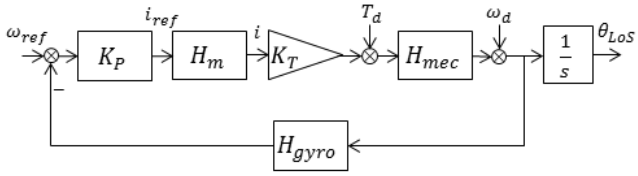

Fig. 2. Block diagram of the studied ISP (single rotational axis)

set to 0. The friction disturbance T_d is modelled as a Dahl friction torque which is representative enough of the friction phenomon observed in the studied system while requiring less coefficients to identify than a LuGre model (see Olsson (1998)). The disturbance input ω_d is a rate disturbance caused by the flexibility of the structure which amplifies part of the vibrating environment. The model includes motor back-EMF, though its influence is strongly reduced by the current loop described below. The output θ_{LoS} is the angular position of the system. Its desired value is taken equal to 0 here.

In what follows, s is the Laplace variable. Note that for sake of confidentality, numerical values are normalized in the sequel: s is divided by a constant.

The actuator is a DC motor. Its current output is controlled in a closed-loop set-up. The current controller is a PID with a roll-off filter whose coefficients will not vary during the tuning process. The transfer function of the closed-loop motor H_m is:

$$H_m(s) = \frac{A(s)}{A(s) + B(s)}, \tag{1}$$

where $A(s) = 0.012(1 + 0.088s)(1 + 0.001s)(1 + 0.126s)$, and $B(s) = (1 + 0.095s)(1 + 0.031s) \times 0.088s \times 0.001s$.

The parameter K_T is the torque constant (0.9 N·m/A) of the motor. The mechanical transfer function comes down to a pure inertia, as shown in (2). Mechanical resonant modes are not taken into account at this stage of the study:

$$H_{mec}(s) = \frac{1}{0.4s}. \tag{2}$$

The gyrometer is modelled as a second-order low-pass filter with a 0.7 damping. A white noise with a Q rad/s/Hz^2 PSD is present up to the gyrometer bandwidth.

Finally, the controller has a transfer function given by:

$$K_P(s) = K \times \frac{1 + aTs}{1 + Ts} \times \frac{\frac{s^2}{\omega_i^2} + \frac{2\xi_i s}{\omega_i} + 1}{s^2 \times (\frac{s^2}{\omega_{ro}^2} + \frac{2\xi_{ro} s}{\omega_{ro}} + 1)}. \tag{3}$$

Among the specifications is the necessity to have a zero steady state error for the angular position in response to a torque disturbance step used as a friction model at first approximation. According to the final value theorem, a double integrator is required in the controller to ensure such a zero position error. A second-order numerator, adjusted with ω_i and ξ_i is added to smooth the influence of the double integrator and preserve sufficient stability margins. The lead phase function obtained by choosing $a > 1$ is used to increase the stability margins. The roll-off filter with parameters ω_{ro} and ξ_{ro} is added to reduce the effect of high-frequency noise and increase the robustness towards neglected dynamics.

The vector $x = [K\ \omega_i\ \xi_i\ a\ T\ \omega_{ro}\ \xi_{ro}]$ gathers the controller parameters to tune.

1.2 The motion MTF

The motion MTF associated with a given controller is calculated using the simulated LoS movements over time and a characteristic time constant τ, related to the integration time or the thermal constant of the optical sensor, depending on the sensor technology. During sequences of duration τ, a Dirac function is animated with the LoS movements on a matrix. This forms a histogram called the Point Spread Function (PSF). The modulus of the PSF Fourier transform is the MTF. As the simulation time of the plant is usually longer than τ, a network of MTFs is obtained. The choice is made here to build one single curve from this network such that ρ percents of the MTFs are above it. This curve will be considered as the motion MTF for the x chosen in the simulated system.

However, this way of evaluating the motion MTF from the LoS movements does not take into account the low-frequency content of the movement. That component creates lag between the different images, which alters the overall visual quality of the output. This lag could be treated by adding a criterion C_d on the movement of the LoS to tune the controller. The criterion is built on the following principle: the human eye has an integration time τ_{eye} of approximately 0.1s (see Holst (2008)). The frame-to-frame motion during this time interval will create blur for the eye. The chosen criterion consists in limiting the peak-to-peak angular motion during intervals of τ_{eye} seconds to half the angular sector seen by one pixel. The very low frequency movement will be seen as a movement of the image and could be dealt with using signal processing.

The LoS controllers are usually tuned on classical control specifications as in Ghaeminezhad et al. (2014) and Roshdy et al. (2012) or on criteria derived from MTF high-level specifications (see ECOM (1975)). These derived criteria may be conservative. The motion MTF is then merely used as a verification tool for already tuned controllers. In this article, the choice is made to build and optimize an image-quality-based criterion including the motion MTF as in Anderson (2010), as well as a criterion C_d to take into account the integration time of the human eye. In the next section, the optimization formulation is described. In section 3, the adopted Bayesian approach is detailed, and in section 4, numerical results are displayed. Section 5 concludes with the results and deals with future works.

2. THE OPTIMIZATION FORMULATION

2.1 The principle of the tuning process

The principle of the tuning process is illustrated in Fig.3

The system described in Fig. 2 is initialized with one point x_0 or a set of N_I points $x_i, i = 1, ..., N_I$ depending on the optimization method employed. A Simulink simulation provides the LoS movement over time for the initial controller(s). A motion MTF is calculated from this movement and fed into the cost function as well as d (the maximum peak-to-peak LoS displacement during intervals of τ_{eye}

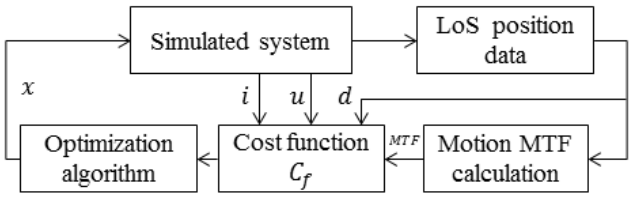

Fig. 3. Principle of the tuning process of the LoS controller

seconds), u and i, respectively the input and the output of the motor. An optimization algorithm then chooses the next set of parameters for the conbtroller K_P. The tuning process goes on until the stopping criterion of the optimization algorithm is met.

2.2 The cost function

The image-quality based cost function consists of two main parts. The first part is formed by the criterion on MTF, C_{MTF}, which accounts for the level of blur introduced into the image during τ and the criterion C_d on frame-to-frame motion. The C_{MTF} idea is to bring the motion MTF above a given reference curve. The motion MTF is discretized in N points over the spatial frequency range and compared to the reference curve. Once the motion MTF is above the reference curve on a particular spatial frequency f_s, C_{MTF} is set to zero for f_s. The idea of C_d is to limit the amplitude of the low-frequency motion of the LoS during τ_{eye}. Once the maximum peak-to-peak angular motion of all sequences of length τ_{eye} is less than half of the Instantaneous Field Of View of the sensor (IFOV), that is to say less than half of the angular sector seen by one pixel, C_d becomes negligible. The second part of the cost function is formed of penalties: as the studied ISP is an on-board system, mean and instantaneous power consumptions are taken into account. Moreover, the controller should ensure stability robustness towards parametrical variations or neglected dynamics. The modulus margin mm is chosen to quantify stability margins. Its expression is:

$$mm = \min_{\omega} \|1 + H_{OL}(j\omega)\| = \frac{1}{\|\frac{1}{1+H_{OL}}\|_{\infty}}, \tag{4}$$

where H_{OL} is the transfer function of the open-loop system.

The calculation of the total cost function is detailed below.

Specifications

- $i_{max} < I_{max}$ with $I_{max} = 2$A
- $p = mean(u \times i) < P$ with $P = 20$W
- $mm > MM$ with $MM = 0.5$
- $d < \frac{1}{2}\theta_0$ with θ_0 the IFOV
- $MTF > MTF_{MIN}$ with MTF_{MIN} the reference curve

Calculation of the cost function

$EV = \max(Re(\text{eigenvalues of the closed-loop system}))$

If $EV < 0$

(1) Simulation of the system
(2) Penalty functions calculation
  - $pen_i = \exp(\frac{i_{max}-I_{max}}{I_{max}})$
  - $pen_p = \exp(\frac{p-P}{P})$
  - $pen_{mm} = \exp(\frac{MM-mm}{MM})$
(3) Image-quality criterion calculation
  - $C_d = \exp(\frac{2d-\theta_0}{\theta_0})$
  - $C_{MTF} = \sum_{i=1}^{N}(MTF_i - MTF_{MINi})_+^2$ with $z_+ = \max(0, z)$
(4) Cost function calculation
  $C_f = -\frac{1}{C_d+C_{MTF}+pen_i+pen_p+pen_{mm}}$

Else $C_f = EV$

2.3 The optimization algorithm

A local optimization algorithm is obviously dependent on the chosen initial point which has to be cleverly designed to hope to be close to the global optimum of the cost function. The choice of a "good" initial candidate requires an experienced control engineer. Moreover, as the cost function may have several local optima, a local optimization algorithm may miss the global optimum.
Using a global optimization algorithm like a genetic algorithm would allow to explore the space of parameters. Evolutionary algorithms have proved efficient in optimizing complex criteria to tune controllers (see Feyel (2013), Sandou (2013)). However, a global algorithm often needs many evaluations of the cost function in order to converge and the more optimization parameters, the higher the number of evaluations needed. Simulating a simplified system and calculating the MTF associated with a given controller takes from 30s up to 1 minute. Taking the population size (P_s =200) and the maximum number of allowed generations (G_a =20) in Anderson (2010), the number of evaluations of the cost function is in the order of magnitude of $P_s \times G_a$. Considering the evaluation time of the cost function to be 30s, running an optimization with a genetic algorithm would take about a day. Increasing the number of parameters of the controller would mean increasing the computational time even more.
Bayesian optimization methods are used to optimize black-box, expensive-to-evaluate functions. It offers the possibility to globally optimize a function with a reduced budget of evaluations by using a surrogate model, while assessing the uncertainty linked with the use of a model.

3. THE BAYESIAN APPROACH

In the Bayesian approach, the cost function C_f is given a prior distribution, in the form of a random process ζ. This prior distribution is combined with previous evaluation results of C_f, $(x_1, C_f(x_1), ..., x_n, C_f(x_n))$, noted F_n, to form a sampling criterion. This criterion is supposed faster to compute than C_f. The maximizer of this sampling criterion is the new evaluation point for C_f, and it will be added to the evaluation results. The algorithm goes on as long as the evaluation budget B of C_f is not exhausted.

The *Expected Improvement* (EI) criterion ρ_n, is chosen to be the sampling criterion. It offers a tradeoff between exploration of the parameter space and exploitation of promising areas while being easily calculable under some assumptions (Jones (1998), chapter 2 in Benassi (2012)). Its definition is given in (5):

$$\rho_n(x) = E_n((m_n - \zeta(X_{n+1}))_+ | X_{n+1} = x), \tag{5}$$

where m_n is the current minimum known value of the cost function and E_n the conditional expectation given F_n.

The random process ζ is chosen to be Gaussian; ζ, conditionned with F_n, has a mean $\hat{\zeta}_n(x)$ and a variance $s_n^2(x)$. One advantage to choose ζ to be Gaussian is that $\hat{\zeta}_n(x)$ and $s_n(x)$ are easy to compute using Kriging theory. Their expressions are given in Jones (2001). Another advantage is the existence of an analytical form for ρ_n (6), expressed with Φ, the normal cumulative distribution function:

$$\rho_n(x) = s_n(x)\Phi'(\tfrac{\delta_n(x)}{s_n(x)}) + \delta_n(x)\Phi(\tfrac{\delta_n(x)}{s_n(x)}) \tag{6}$$

with $\delta_n(x) = m_n - \hat{\zeta}_n(x)$, the improvement with respect to the current minimum.

The principle of the approach is summed up in Fig.4.

In practice, a covariance function k for ζ has to be defined. As information on C_f is not readily available, the covariance function is taken in a parametrized class of covariance functions. The class of Matérn covariance functions is chosen for this paper. The Matérn covariance functions are widely used in Bayesian kriging methods because of the possibility they offer to model a wide class of problems (Pilz (2008)). The measure of the distance between two vectors of parameters x^a and x^b is noted h:

$$h(x^a, x^b) = \sqrt{\sum_{i=1}^{D} \frac{(x_i^a - x_i^b)^2}{\beta_i^2}}, \tag{7}$$

where D is the length of x^a and x^b and is equal to 7 here.

The positive scalars β_i are range parameters of the covariance, that is to say characteristic correlation lengths: the smaller the β_i, the more the cost function is supposed likely to vary in the ith direction.

The covariance function k is given by:

$$k(x^a, x^b) = \frac{\sigma^2}{2^{\nu-1}\Gamma(\nu)}(2\nu^{1/2}h)^\nu \mathcal{K}_\nu(2\nu^{1/2}h), \tag{8}$$

where, for the sake of conciseness, $h(x^a, x^b)$ is abbreviated in h.

Γ represents the Gamma function and $\mathcal{K}_\nu$ is the modified Bessel function of the second kind, of order ν. σ^2 is a variance parameter. The parameter ν is linked with the smoothness of the cost function. The parameter ν is chosen fixed here, equal to the usual value of 5/2.

The parameters $(\sigma, \beta_1, ..., \beta_D)$ are estimated by restricted maximum likelihood of the observed data (see Santner et al. (2003) for more details on the restricted maximum likelihood). This estimation is performed after each new evaluation of the cost function C_f, according to the principle of the EGO algorithm (see Jones (1998)).

The Kriging operations to compute $\hat{\zeta}_n(x)$ and $s_n(x)$, as well as the estimation of the parameters $(\sigma, \beta_1, ..., \beta_D)$ are performed with *STK* (see Bect, Vazquez et al. (2014)), that can be distributed and modified under the terms of the GPLv3 licence.

For more details on Kriging and on the Bayesian approach, see Jones (1998), Benassi (2012) and references therein.

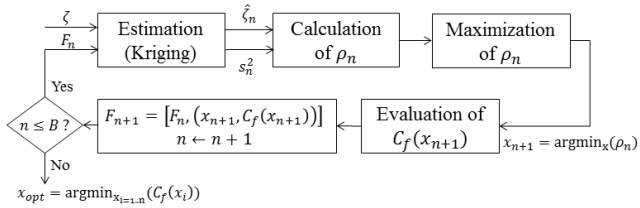

Fig. 4. Principle of the Bayesian optimization

The EI criterion has to be maximized to find the next evaluation point of C_f. Several methods, listed in chapter 4 of Benassi (2012) have been tested on this problem. The method presented here was chosen for its ease of implementation: the EI criterion is simply maximized over a maximin Latin Hypercube Sampling (maximin LHS) grid of 10^5 points. Details on the maximin LHS are given in Santner et al. (2003). The chosen number of points in the grid is a tradeoff between representativity and available computer memory. A local optimization, using the Matlab *fmincon* interior-point algorithm is then launched, initialized with the best point found on the grid. The next point of evaluation of C_f is the best point found by the local optimization of the EI criterion.

4. NUMERICAL RESULTS

The initial design is a maximin LHS grid. Usually, the number of points included in the initial design is equal to 10 times the dimension of the optimization parameters (see Benassi (2012)). Thus, here, the initial LHS grid consists of 70 points. 500 evaluations of the cost function are further allowed in the budget of evaluations B. The results of the optimization are compared with the result of a local optimization method, previously presented in (Frasnedo (2015)). The aim of the local optimization was to use the image-quality based criterion to improve a "good" controller, tuned beforehand on classic control specifications. This method will be named "Method 1" whereas "Method 2" will refer to the global optimization algorithm using a Bayesian approach, which is run without any knowledge of an initial available controller.

The final set of parameters x_{M1} of the controller optimized by using Method 1 is given by:

$$x_{M1} = [43880\ 0.30\ 0.89\ 1.8\ 0.377\ 274\ 0.73]. \tag{9}$$

The final set of parameters x_{M2} of the controller optimized by using Method 2 is given by (10):

$$x_{M2} = [45068\ 0.27\ 0.33\ 1.15\ 0.297\ 62\ 0.33]. \tag{10}$$

x_{M1} and x_{M2} coefficients are close, except for the roll-off pulsation ω_{ro}, which is lower in the vector of parameters found by Method 2 and the damping coefficients ξ_i and ξ_{ro}.

The MTFs of both systems respect the requirement of being above the reference curve (see Fig. 5). The MTF of the system with the controller tuned by Method 2 (noted $MTF2$) is slightly better than the MTF of the system whose controller was tuned by Method 1 (noted $MTF1$). The level of blur resulting from the LoS movement during the time constant τ of the sensor is thus lower with the controller optimized by Method 2.

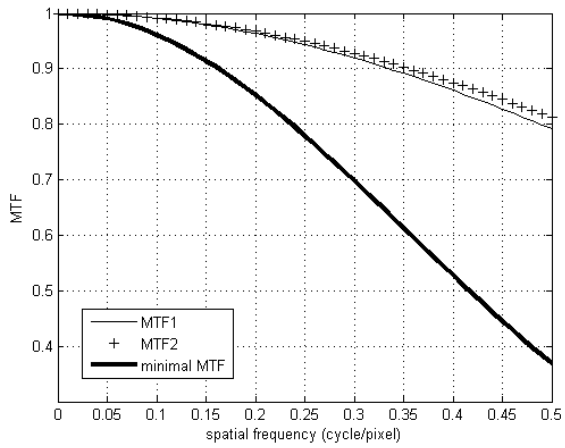

Fig. 5. $MTF1$ and $MTF2$ and the reference MTF over spatial frequency

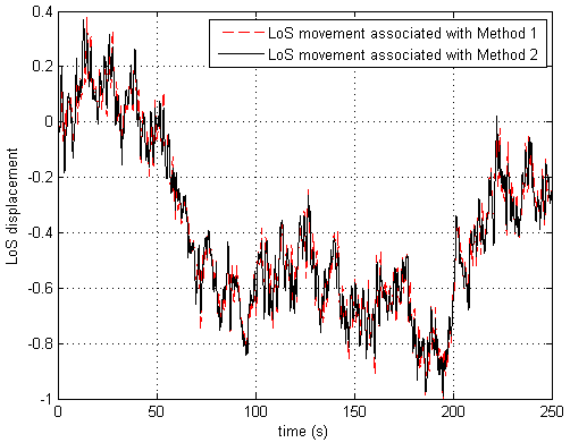

Fig. 6. LoS movements associated with Method 1 and Method 2 over time

Image quality for the human eye is also impacted by the frame-to-frame motion during the integration time τ_{eye}. The LoS displacements associated with the controller issued from Method 1 and with the controller issued from Method 2 are displayed in Fig. 6. In this stabilization problem, the θ_{LoS} desired value is arbitrarily taken to 0. The displacements shown in Fig. 6 thus represent the position error over time. The difference between LoS movements associated with Method 1 and Method 2 is represented in Fig. 7 (note that the amplitude of the LoS movements is normalized for confidentiality reasons in Fig. 6 and Fig. 7). The initial controller used to initialize Method 1 strongly violated the specification on maximum peak-to-peak movement with d equal to $7.3\frac{\theta_0}{2}$ instead of the desired $\frac{\theta_0}{2}$. The final controller significantly reduced the gap between the obtained value for d and the specified value (see Frasnedo (2015)). Though the controller optimized through Method 2 still does not comply with the given specification on d, it further reduces this gap (see table 1).

Both controllers comply with the constraint on the stability margin. The open-loop system with parameters x_{M1} and the open-loop system with parameters x_{M2} are repre-

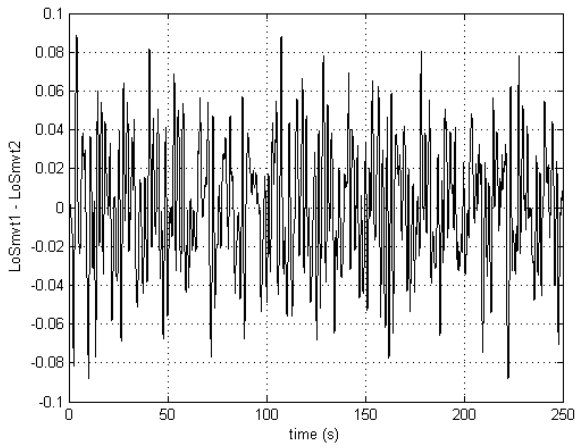

Fig. 7. Difference between LoS movements associated with Method 1 and with Method 2 over time

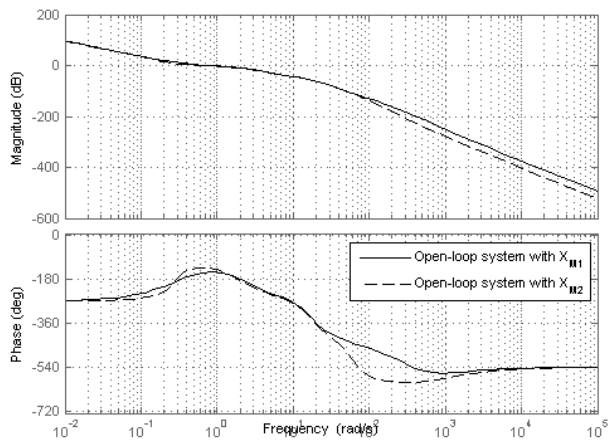

Fig. 8. Open-loop system with x_{M1} controller and open-loop system with x_{M2} controller

sented in Fig. 8. The gain and phase margin are displayed in Fig. 9: the gain margin is equal to 9.37dB and the phase margin is equal to 29.9 degrees for the open-loop system with the x_{M1} controller while the x_{M2} controller allows a 5.82 dB gain margin and a 43.4 degrees phase margin. On the whole, the x_{M2} controller allows a better modulus margin than the x_{M1} controller (see table 1).

The instantaneous power consumption, measured by i_{max} and the mean power consumption, quantified by p are below the constraints in both cases (see table 1).

The execution time of Method 1 is 3h10 on an Intel(R) Core(TM) i7-26005 CPU (2.8GHz), with 378 evaluations of the cost function. The execution time of Method 2 is 2h40 on the same computer, with 570 evaluations of the cost function. The fact that more evaluations of the

Table 1. Penalty and image criteria values

Penalties and image criteria	Goal	Method 1	Method 2
i_{max}	<2A	0.36 A	0.33 A
mm	>0.5	0.50	0.52
p	<20W	0.07 W	0.07 W
d	$< \frac{1}{2}\theta_0$	$1.8\times\frac{\theta_0}{2}$	$1.6\times\frac{\theta_0}{2}$
C_{MTF}	0	0	0

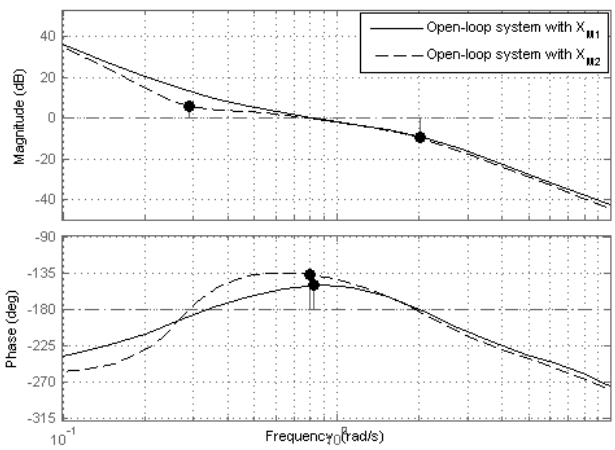

Fig. 9. Gain and phase margins with x_{M1} controller and with x_{M2} controller

cost function have been carried out with Method 2 within less time than with Method 1 can be simply explained: when the algorithm finds a controller that stabilizes the system, "expensive" operations are launched (the Simulink simulation of the system and the calculation of the motion MTF) whereas it is not the case when the controlled system is not stable. In the first case, 347 evaluations over 378 represent stabilizing controllers. In the second case, among the 570 evaluations of the cost function, only 143 of them turn out to be stabilizing controllers. Method 2 explores the space of parameters and finally produces a better controller in terms of cost function (see table 1) than Method 1.

5. CONCLUSION

A method to globally optimize the position controller of an ISP on an image-quality-based criterion has been presented. The final controller complies with the constraints on power consumption and stability. Regarding the image-quality-based performances, the controller reaches better levels than a controller tuned with a local optimization method, while taking less time to tune. Moreover, the optimization method based on a Bayesian approach does not need to be initialized with an acceptable point, that has been previously tuned by a control engineer. The results seem promising and show the interest of the approach in terms of computational time and quality of the solution. However the specification on d is not reached whereas the specification on MTF is largely met. In order to satisfy both specifications, the next step could be to reformulate the optimization problem as a multi-objective problem. Another step could be to work with a more complex controller, involving more parameters.

REFERENCES

D. Anderson. Evolutionary algorithms in airborne surveillance systems: image enhancement via optimal sightline control. *Journal of Mechanical Engineering Science*, volume 225, Issue 10, 2010, pages 1097–1108.

J. Bect, E. Vazquez. *STK: a Small (Matlab/Octave) Toolbox for Kriging.* Release 2.2.0. Toolbox available at `http://kriging.sourceforge.net`.

R. Benassi. Nouvel algorithme d'optimisation bayésien utilisant une approche Monte-Carlo séquentielle. PhD thesis, Supélec 2012.

United States Army Electronics Command (ECOM). *Night Vision Laboratory Static Performance Model for Thermal Viewing Systems.* National Technical Information Service, 1975, page 10.

Ph. Feyel, G. Duc, G. Sandou. LuGre friction model identification and compensator tuning using a Differential Evolution algorithm. *IEEE Symposium on Differential Evolution (SDE)*, Singapore, 2013, pages 85–91.

S. Frasnedo, C. Chapuis, G. Duc, Ph. Feyel, G. Sandou. Line of sight stabilization controllers tuning from high-level Modulation Transfer Function specifications. *Workshop on Advanced Control and Navigation for Autonomous Aeroespace Vehicles*, Seville, Spain, 2015 (to appear).

N. Ghaeminezhad, W. Daobo, and F. Farooq. Stabilizing a Gimbal Platform using Self-Tuning Fuzzy PID Controller. *International Journal of Computer Applications*, volume 93, No 16, 2014.

J. M. Hilkert. Inertially Stabilized Platform Technology, concepts and principles. *IEEE Control Systems magazine*, volume 28, Issue 1, 2008, pages 26–46.

G. C. Holst. *Electro-Optical Imaging System performance.* JCD Pub. and SPIE Optical Engineering Press, Bellingham, Wash., 4th edition 2008 - 442 pages.

D. R. Jones, M. Schonlau, W. J. Welch Efficient global optimization of expensive black-box functions. *Journal of Global Optimization*, volume 13, Issue 4, 1998, pages 455–492.

D. R. Jones. A Taxonomy of Global Optimization Methods Based on Response Rurfaces. *Journal of Global Optimization*, volume 21, Issue 4, 2001, pages 343–383.

H. Olsson, K. J. Åström, C. Canudas de Wit, M. Gäfvert, P. Lischinsky. Friction Models and Friction Compensation. *European Journal of Control*, volume 4, Issue 3, 1998, pages 176–195.

J. Pilz, G. Spöck. Why do we need and how should we implement Bayesian kriging methods. *Stochastic Environmental Research and Risk Assessment*, volume 22, Issue 5, 2012, pages 621–632.

A. A. Roshdy, C. Su, H. F. Mokbel, Y. Z. Lin, and T. Wang. Design a robust PI controller for Line of Sight stabilization system. *International Journal of Modern Engineering Research*, volume 2, Issue 2, 2012, pages 144–148.

G. Sandou. *Metaheuristic Optimization for the Design of Automatic Control Laws.* Hermes Science Publications, 2013 - 152 pages.

T. J. Santner, B. J. Williams, W. I. Notz. *The Design and Analysis of Computer Experiments.* Springer Science & Business Media, 2003 - 283 pages.